
This is an electronic reprint of the original article.
This reprint may differ from the original in pagination and typographic detail.

Weckman, Timo; Laasonen, Kari

Atomic Layer Deposition of Zinc Oxide: Study on the Water Pulse Reactions from First Principles

Published in:
Journal of Physical Chemistry C

DOI:
[10.1021/acs.jpcc.7b11469](https://doi.org/10.1021/acs.jpcc.7b11469)

Published: 01/01/2018

Document Version
Publisher's PDF, also known as Version of record

Published under the following license:
CC BY

Please cite the original version:
Weckman, T., & Laasonen, K. (2018). Atomic Layer Deposition of Zinc Oxide: Study on the Water Pulse Reactions from First Principles. *Journal of Physical Chemistry C*, 122(14), 7685–7694.
<https://doi.org/10.1021/acs.jpcc.7b11469>

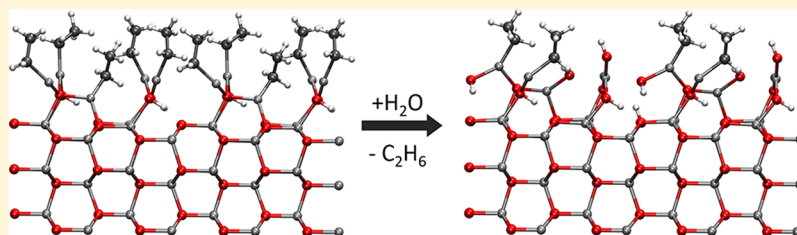
This material is protected by copyright and other intellectual property rights, and duplication or sale of all or part of any of the repository collections is not permitted, except that material may be duplicated by you for your research use or educational purposes in electronic or print form. You must obtain permission for any other use. Electronic or print copies may not be offered, whether for sale or otherwise to anyone who is not an authorised user.

Atomic Layer Deposition of Zinc Oxide: Study on the Water Pulse Reactions from First-Principles

Timo Weckman¹ and Kari Laasonen^{1*}

Department of Chemistry and Materials Science, School of Chemical Engineering, Aalto University, Espoo 00076, Finland

Supporting Information



ABSTRACT: Atomic layer deposition (ALD) of zinc oxide thin films has been under intense research in the past few years. The most common precursors used in this process are diethyl zinc (DEZ) and water. The surface chemistry related to the growth of a zinc oxide thin film via atomic layer deposition is not entirely clear, and the ideal model of the process has been contradicted by experimental data, e.g., the incomplete elimination of the ethyl ligands from the surface and the non-negative mass change during the water pulse. In this work we investigate the surface reactions of water during the atomic layer deposition of zinc oxide. The adsorption and ligand-exchange reactions of water are studied on ethyl-saturated surface structures to grasp the relevant surface chemistry contributing to the deposition process. The complex ethyl-saturated surface structures are adopted from a previous publication on the DEZ/H₂O-process, and different configurations are sampled using *ab initio* molecular dynamics in order to find a suitable minimum structure. Water molecules are found to adsorb exothermically onto the ethyl-covered surface at all the ethyl concentrations considered. We do not observe an adsorption barrier for water at 0 K; however, the adsorption energy for any additional water molecules decreases rapidly at high ethyl concentrations. Ligand-exchange reactions are studied at various surface ethyl coverages. The water pulse ligand-exchange reactions have overall larger activation energies than surface reactions for diethyl zinc pulse. For some of the configurations considered, the reaction barriers may be inaccessible at the process conditions, suggesting that some ligands may be inert toward ligand-exchange with water. The activation energies for the surface reactions show only a weak dependence on the surface ethyl concentration. The sensitivity of the adsorption of water at high ethyl coverages suggests that at high ligand-coverages the kinetics may be somewhat hindered due to steric effects. Calculations on the ethyl-covered surfaces are compared to a simple model containing a single monoethyl zinc group. The calculated activation energy for this model is in line with calculations done on the complex model, but the adsorption of water is poorly described. The weak adsorption bond onto a single monoethyl zinc is probably due to a cooperative effect between the surface zinc atoms. A cooperative effect between water molecules is also observed; however, the effect on the activation energies is not as significant as has been reported for other ALD processes.

INTRODUCTION

Thin film growth using atomic layer deposition (ALD) has become an important manufacturing process in nanotechnology within the recent decade, driven by the decreasing dimensions of modern technology. ALD is based on sequential, self-limiting gas–solid reactions.¹ The resulting films are uniform and pinhole free, and the process allows the film thickness to be controlled at the atomic level. In ALD, the reactants, precursors, are introduced into the reactor chamber separately, thus avoiding any gas-phase reactions. All the chemical reactions are restricted to take place on the surface as the reactor chamber is purged with inert gas between alternating reactant pulses.

Zinc oxide is a wide band gap semiconductor with several interesting properties,^{2–4} for example, high transparency, tunable electrical conductivity, and piezoelectric properties.

The zinc oxide thin films have been used in various applications, for example, in transistors, solar cells, and sensors. The interest in deposition of zinc oxide thin films using ALD has increased as the dimensions of microscopic devices have decreased.

The most common precursors used to deposit zinc oxide thin films via ALD include diethyl zinc (DEZ) and water. The thin film growth of zinc oxide using these precursors is the focus of our present study.

The temperatures usually used in deposition of zinc oxide range from 100 to 200 °C. The as-deposited thin films are polycrystalline with various lattice orientations present, and

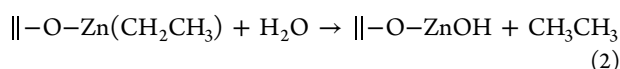
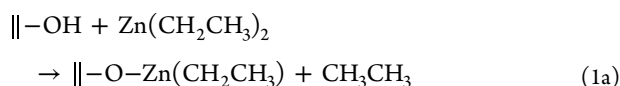
Received: November 21, 2017

Revised: February 19, 2018

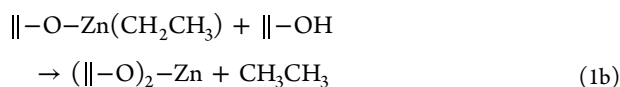
Published: March 22, 2018

these orientations are sensitive to temperature. At low and high deposition temperatures (below 100 °C and above 200 °C) the (002) orientation is dominant. However, the (002) orientation diminishes between temperatures 100 and 200 °C and the (100) orientation becomes slowly dominant, reaching its peak at 160–200 °C.^{5–7} We have therefore selected the (100) surface as the substrate for our computational study. The growth-per-cycle (GPC) for the zinc oxide ALD-process ranges from 1.7 to 2.1 Å depending on the temperature.⁸

The assumed reaction mechanisms for the DEZ/H₂O-process are



Thus, the main reactions are assumed to be the adsorption of a DEZ with the loss of one of its ligands (eq 1a) and a subsequent reaction between the monoethyl zinc (MEZ) and water during the water pulse (eq 2). The monoethyl zinc may also react further on the surface to produce a bare zinc on the surface:



The mechanism in eq 1b is usually omitted in experimental publications, and the dominant end-product from the DEZ pulse is assumed to be MEZ. After the surface has been saturated with DEZ, it is assumed that all the surface ethyl ligands are removed during the subsequent water pulse resulting in a hydroxylated surface at the end of the ALD cycle.^{8,9} Assuming that the main product from the DEZ pulse is monoethyl zinc, then the overall reaction would lead to a clearly negative mass change at the end of the water pulse since the ethyl ligand is replaced by a much lighter hydroxyl group. However, the mass change measured using a quartz-crystal mass-balance (QCM)⁸ is slightly positive during the water pulse. One proposed explanation for this is the presence of bare zinc atoms on the surface in addition to the monoethyl zinc groups. These bare zinc sites could adsorb more water onto the surface and balance out the mass change from the ligand-exchange reaction. Ferguson et al.¹⁰ have suggested the pyrolysis of diethyl zinc to result in bare surface zinc atoms.

The commonly made assumption that all the surface ethyl ligands are removed from the surface after the water pulse has been shown to be incorrect by Mackus et al.¹¹ The authors conducted an *in situ* gas-phase and surface FTIR spectroscopy measurements on the ALD of zinc tin oxide (ZTO) thin films and note that after a typical water exposure 30–50% of the surface ethyl ligands remain on the surface during the growth of a ZnO thin film. Even after extended periods of water exposure, approximately 16% of surface ethyl ligands remain on the surface at 150 °C temperature, and only at elevated temperatures around 200 °C have virtually all the ligands been removed from the surface. The authors conclude that there is a high kinetic barrier for removing some of the ligands from the surface during the water pulse.

There have previously been only a few computational papers on the growth of zinc oxide with ALD. Afshar and Cadien¹² used a cluster model to simulate the ZnO ALD process and

reported the activation energies for the DEZ and H₂O half-reactions on the surface to be 1.34 and 1.83 eV, respectively. Ren¹³ used a similar cluster model to investigate the heterodeposition of ZnO on Si(100) substrate. On the Si(100) substrate, the removal of the first ligand from DEZ had a barrier ranging from 0.47 to 0.67 eV for the removal of the first ligand and 1.70 eV for the second ligand. The barrier for a reaction between a monoethyl zinc and a water molecule was calculated to be 1.21 eV.

In our recent study on the surface reactions of diethyl zinc on a hydroxylated (100) zinc oxide surface,¹⁴ we conclude that the activation energy for the ligand-exchange reaction between adsorbed diethyl zinc and a surface hydroxyl group/molecular water is low, ranging from 0.23 to 0.47 eV on the planar surface. We denote this first ligand-exchange reaction as LE1. This barrier was observed to be higher in calculations done on a stepped surface where the barrier rose to 0.90–0.93 eV. A proposed pyrolysis mechanism of diethyl zinc was also investigated, but based on our calculations the pyrolysis of ethyl ligands to form butane has a large barrier of 1.96 eV. The pyrolysis is therefore unlikely to contribute to the growth of the thin film.

The activation energy for the removal of the final ligand from the monoethyl zinc was considerably high. We denote this mechanism as LE2. On the planar surface the barrier for the reaction with a monoethyl zinc and a hydroxyl group ranged from 1.31 to 1.52 eV. However, a lower barrier for this reaction was found on a surface step where the monoethyl zinc was three-coordinated. In this case the barrier for the reaction was only 0.95 eV. Instead of the pyrolysis mechanism, the second ligand-exchange reaction may produce bare zinc atoms onto the surface, and this can partially explain the positive mass change during the water pulse as more water can adsorb onto the surface zinc atoms resulting in a stoichiometric film.

Two different ethyl-saturated surface structures were constructed.¹⁴ A low temperature estimate was obtained assuming that the second ligand-exchange reaction (mechanism in eq 1b) is not accessible in the process conditions, thus leading to monoethyl zinc-saturated surface with some hydroxyl groups present (case 1 structure). For the high temperature estimate we assumed that the second ligand-exchange can also occur and the amount of hydroxyl groups on the surface becomes the limiting factor. This leads to a combination of both monoethyl zinc and bare zinc atoms on the surface (case 2 structure).

To understand the overall growth process, one must study both precursor pulses. In a common computational study on an ALD-process, the follow-up calculations for the second precursor pulse usually omit the complexity of the surface structure after saturation by the previous precursor. In this work we investigate surface reactions relevant for the water pulse using the ethyl-saturated structures from our previous publication and address the discrepancies between the ideal model and experimental data from an atomic-scale perspective. The structure of the ethyl-covered surface is not as well-defined as that of an ideal hydroxylated oxide surface, because of more degrees of freedom in finding a suitable minimum energy structure. To overcome this enormous complexity, we propose that a sequence of reactions on complex surface environments can produce a reasonable range of possible surface processes that contribute to the growth of the thin film. We also study the effects that water–water interactions may play on the surface reactions in stabilizing the transition states and decreasing the

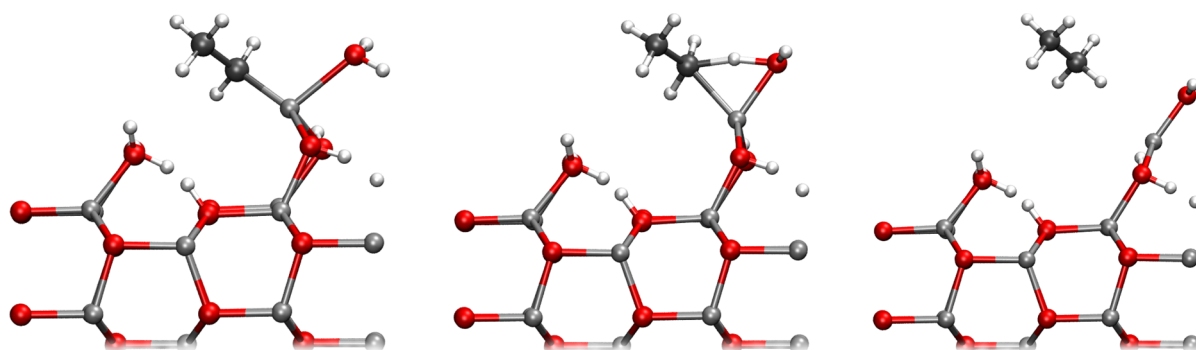


Figure 1. Initial, transition, and final states for the ligand-exchange reaction between the isolated monoethyl zinc site and a single water molecule.

activation energy and investigate ethyl pyrolysis on the surface via radical formation and β -elimination to comprehensively explore other proposed reactions pathways.

■ COMPUTATIONAL METHODS

The reaction pathways were studied using density functional theory as implemented in GPAW.¹⁵ The Perdew–Burke–Ernzerhof (PBE) exchange and correlation functional¹⁶ was used with grid spacing of 0.2 Å. The PBE functional has been previously used in studies on the zinc oxide surface chemistry and has been shown to produce reasonable results.^{17,18} The TS09 van der Waals correction was used on top of the PBE functional as proposed by Tkatchenko and Scheffler¹⁹ to include the weak dispersion interactions between ethyl ligands.

The k-points sampling of the reciprocal space was done using a $2 \times 2 \times 1$ Monkhorst–Pack grid. All geometry optimizations were carried out to gradients smaller than 0.05 eV/Å. The calculations were conducted in a 2×2 primitive cell simulation box. The surface slab had six stoichiometric oxide layers as in our previous study.¹⁴ All of the barriers presented in the results have been calculated using the nudged elastic band method with climbing image.²⁰

Some short Born–Oppenheimer molecular dynamics simulations were carried out to find a suitable minimum on the potential energy surface (PES). Dynamic simulations were carried out using a small polarized double- ζ basis set and a Berendsen thermostat at 450 K.

■ RESULTS

While the surface structure of a hydroxylated (100) zinc oxide surface is rather well-defined with only few possible configurations to explore, the minimum energy structure of the ethyl-saturated surface of zinc oxide is not unambiguous because of the tremendous increase in the degrees of freedom. Therefore, two approaches were taken to investigate the surface reactions during the water pulse. First, we studied the adsorption and ligand-exchange reaction of a single water molecule on an isolated monoethyl zinc site on the planar zinc oxide (100) surface. Using a single reactive site to represent the surface reaction is an approach commonly used in *ab initio* surface studies. Second, we studied water molecules on the two different ethyl-saturated surface structures representing the zinc oxide surface after the DEZ pulse.

All the adsorption structures for water on the saturated structures presented below were produced by first inserting a single molecule onto some suitable adsorption site (i.e., close to a monoethyl zinc or a bare zinc on the surface). A short NVT *ab initio* molecular dynamics (AIMD) simulation was run for

1.5 ps at 450 K to allow the system to explore the potential energy surface. From this trajectory, few snapshots at fixed intervals were taken and optimized, and the lowest energy configuration was chosen as the starting point for a ligand-exchange reaction. The transition state was located using the nudged elastic band (NEB) method. After the reaction, the newly formed ethane molecule was removed, and another short AIMD simulation was run as described above. This allows the system to relax after the ligand had been removed. The procedure was repeated for all the configurations.

Water Pulse Reactions with an Isolated Monoethyl Zinc. The common approach to surface chemistry is to study specific chemical reactions on isolated sites on a surface or an atomic cluster representing a surface. These types of calculations have significant benefits as the minimum energy structure is usually well-defined for a small system, and one can get a reasonable estimation for the activation energy of the surface reaction. The specific variables (bonding, coordination number, etc.) can usually be varied independently. However, these types of models neglect the effects caused by large surface coverage, e.g., steric effects or change in the surface acidity. In order to estimate the extent of these effects and to produce calculations comparable to other computational publications in the literature (i.e., other precursors and cluster model type calculations), we have conducted calculations between a single water molecule and a monoethyl zinc on a hydroxylated zinc oxide (100) surface as an idealized model for the water pulse reaction.

The water adsorption and ligand-exchange reaction was studied on a monoethyl zinc bridged between two oxygens on the (100) surface. This structure is obtained from a ligand-exchange reaction between a diethyl zinc and a surface hydroxyl group.¹⁴ The monoethyl zinc is rather inert with respect to a ligand-exchange reaction with a surface hydroxyl group as the activation energy for this reaction ranges from 1.31 to 1.52 eV depending on the surface ethyl concentration.

To study the water pulse mechanism we placed a water molecule onto the zinc atom of the monoethyl zinc group. The adsorption bond between the water molecule and the zinc atom is weak with a bond energy of -0.36 eV. The weak bond is reflected also in the lengthy adsorption bond of 2.29 Å between the zinc and the oxygen.

The adsorbed water can donate a proton to the ethyl ligand producing ethane as shown in Figure 1. The transition state is 0.96 eV above the adsorbed state in energy. The O–Zn bond length decreases to 2.05 Å, close the bulk value in the transition state. The Zn–C bond increases from 1.97 to 2.24 Å, and the O–H and C–H bond lengths are 1.28 and 1.43 Å, respectively.

Table 1. Adsorption Energies, Reaction Barriers, and Reaction Energies for the Adsorption and Ligand-Exchange Reactions for Water on Ethyl-Saturated Zinc Oxide Surfaces^a

reaction	MEZ	H ₂ O	E_{ads}	E_{act}	ΔE	cn_{Zn}	cn_{O}	$d_{\text{Zn-O}}$	
C1-5MEZ-1H ₂ O	5	1	-1.21	1.15	0.18	2	1	3.42	*
C1-4MEZ-2H ₂ O	4	2	-0.79	0.96	-0.26	2	1	3.80	
C1-3MEZ-3H ₂ O	3	3	-0.99	1.00	0.02	2	1	3.56	
C1-2MEZ-4H ₂ O	2	4	-1.76	1.39	-0.42	2	2	4.35	*
C1-1MEZ-5H ₂ O	1	5	-1.63	1.22	-0.19	3	3	2.19	*
C2-4MEZ-1H ₂ O	4	1	-1.07	1.31	0.04	2	2	2.21	*
C2-3MEZ-2H ₂ O	3	2	-2.32	1.26	-0.81	3	3	2.17	*
C2-2MEZ-3H ₂ O	2	3	-1.03	0.93	0.76	2	2	3.47	*
C2-1MEZ-4H ₂ O	1	4	-1.26	1.56	-0.93	3	1	3.27	*

^aThe mechanisms where the reacting oxygen group was a hydroxyl group instead of a water molecule are designated with an asterisk. cn_{Zn} and cn_{O} are the coordination numbers for the reacting zinc and oxygen atoms, respectively, at the initial configuration. The coordination number is defined as the number of zinc/oxygen atoms within 2.5 Å cutoff from the selected atom. The distance $d_{\text{Zn-O}}$ describes the distance between the Zn atom of the monoethyl zinc and the oxygen of the water/hydroxyl group in angstroms at the initial configuration. The energies are given in eV.

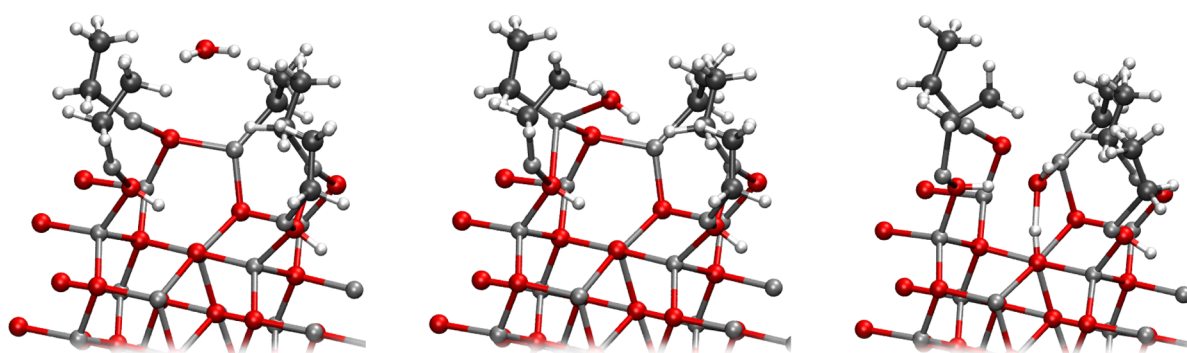


Figure 2. Water molecule is able to approach the surface with no barrier. The optimal adsorption site is the zinc atom of a monoethyl zinc group, where the water is able to form a hydrogen bond with a surface hydroxyl group (right). In our calculated trajectory, the water molecule has a metastable intermediate state 0.25 eV above the optimal site (middle), where the water is bonded to another monoethyl zinc group. We find no barrier of significance for adsorption.

In the final configuration the zinc atom is three-coordinated with two bonds to the surface oxygens and one to the new hydroxyl group from the adsorbed water molecule.

A slight increase in the surface monoethyl zinc coverage did not have an effect on the energetics of the ligand-exchange reaction. A second monoethyl zinc was added between the two free oxygen sites on the surface. The adsorption energy for the water was -0.40 eV, and the barrier for the ligand-exchange reaction was 1.01 eV, close to the barrier with only one monoethyl zinc. The difference in the barrier is equal to the change in the adsorption energy. There were only slight deviations in the bond lengths at the transition state.

The adsorbed water molecule had only a slight effect on the reaction barrier for the ligand-exchange reaction between the monoethyl zinc and a surface hydroxyl group. With the water molecule bonded to the monoethyl zinc, the energy of the activated complex is 1.34 eV, while the activation energy for the single monoethyl zinc reported in our previous study was 1.42 eV.¹⁴

Water Pulse on Ethyl-Terminated Surface. In the case of an ALD process, the surface composition is determined by the previous precursor, in this instance the diethyl zinc. We used the two monoethyl zinc-saturated surfaces presented in our previous publication¹⁴ to study the adsorption and ligand-exchange reactions of water on a realistic chemical environment. These two structures correspond to low and high temperature limits for the DEZ-saturated surfaces, and we have labeled them cases 1 and 2, respectively.

The diethyl zinc has two ligands, and the removal of the first ligand has a low barrier (<0.5 eV). However, the second ligand is not as easily removed, and the calculated barriers for this mechanism range from 0.95 to 1.59 eV. On the basis of the fact that DEZ reacts with two processes, one fast and the other one slow, two estimations for the ethyl-saturated surface were constructed. In generating the case 1 structure, it is assumed that at low temperature DEZ can lose only one of its ethyl ligands via ligand-exchange with a hydroxyl group. This leads to a monoethyl zinc-saturated surface, and the limiting factor becomes the steric hindrance between the surface ethyl ligands. The case 2 structure was obtained by assuming that at elevated temperatures the monoethyl zinc can also react with a surface hydroxyl group through the slower process. This leads to a mixture of bare zinc atoms and monoethyl zinc groups, and the amount of hydrogen on the surface becomes an additional limiting factor.

Series of calculations were conducted on both saturated structures by placing one water molecule at a time onto the surface, and a short *ab initio* molecular dynamics simulation was conducted. Snapshots with a fixed interval were chosen from the dynamic trajectory for optimization. The lowest energy configuration was taken as the initial configuration for a ligand-exchange reaction. The reaction was calculated between a hydroxyl/water molecule and an ethyl site deemed the most suitable for a reaction. The transition state for the ligand-exchange reaction was calculated using the NEB method. After the reaction the ethane molecule was removed from the system,

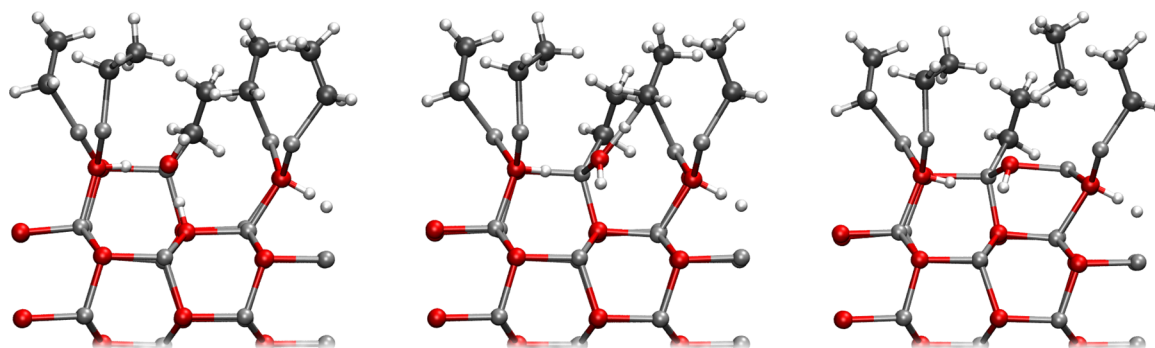


Figure 3. Initial, transition, and final states for the reaction mechanism C1-5MEZ-1H₂O.

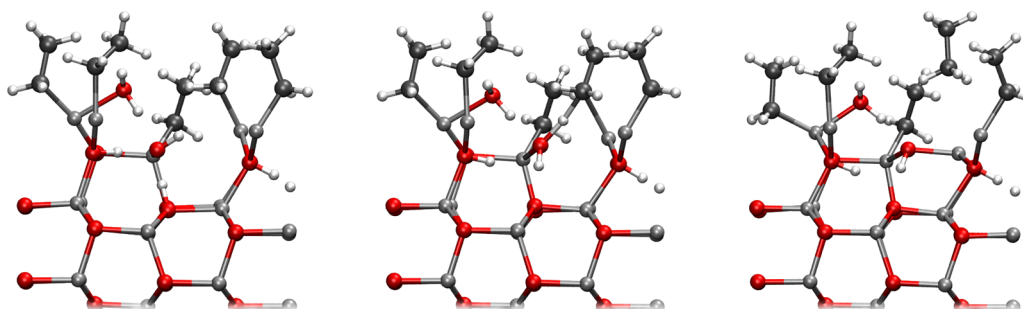


Figure 4. Initial, transition, and final states for the reaction mechanism C1-5MEZ-2H₂O. The reaction mechanism is the same as for C2-5MEZ-1H₂O with additional water forming a hydrogen bond to the reacting hydroxyl group.

and another molecular dynamic simulation and optimization were conducted to find a reasonable starting configuration for the adsorption of the next molecule. The trajectories for these different ligand-exchange reaction mechanisms are provided in the [Supporting Information](#).

The calculations on these saturated structures present, by no means, a comprehensive investigation of all the possible reaction pathways on the surface. We propose that looking at multiple surface reactions on these complex surface structures gives us a reasonable grasp of the range of activation energies that the surface reactions can have. The energetics of different mechanisms on the two saturated surface structures are presented in [Table 1](#). The reactions are labeled with an acronym *Cl-nMEZ-mH₂O*, representing the case *l* = 1, 2 surface with *n* monoethyl zinc groups and *m* H₂O molecules. For example, the structure C1-5MEZ-1H₂O is the case 1 structure with five ethyl ligands on the surface and one water molecule.

As a case study, let us look at the adsorption and the surface reaction of a single water molecule on the case 1 structure. The case 1 saturated structure has five ethyl ligands in the simulation box and has the highest ethyl-ligand concentration of all the structures. Therefore, it was used to investigate the adsorption of the water molecule in closer detail. To look for a possible barrier for adsorption, the adsorption pathway was explored from above the ethyl ligands (i.e., the gas-phase) to the adsorption site. The trajectory was optimized using the NEB method. The adsorption pathway is illustrated in [Figure 2](#). The water molecule is able to approach the surface without being blocked by the other ethyl ligands, and no barrier was found for this pathway. The lowest energy configuration was found when the water molecule was bonded to the zinc atom of a monoethyl zinc group while forming a hydrogen bond with a surface oxygen. The water molecule dissociates by donating a proton to a surface oxygen. A local minimum configuration

exists about halfway along the calculated path, where the water is bonded to a zinc atom of another monoethyl zinc group, slightly above where the optimal site is. The energy difference between these two sites is 0.25 eV with a negligible barrier of 0.07 eV between.

The adsorption bond between the water molecule and the monoethyl zinc group is strong with adsorption energy of -1.21 eV. The Zn–O bond length is 2.02 Å, close to a bulk value. Since we were not able to see any significant barrier for the adsorption of water onto the surface, we assume that there is no significant barrier for adsorption of water in any of the other configurations discussed, since the ethyl concentration is lower in these configurations.

The adsorbed water molecule dissociates by sharing a proton with a bare surface oxygen atom. From here the water molecule can react with an ethyl ligand by donating a proton to the ligand and producing an ethane molecule. The ligand-exchange reaction was not calculated with the monoethyl zinc to which the water was adsorbed but between the water and a neighboring surface monoethyl zinc (see [Figure 3](#)) as this ethyl ligand can more easily accept the proton. At the transition state, the Zn–O bond remains quite stable at 2.04 Å and the Zn–C bond increases from 1.98 to 2.18 Å. The C–H and O–H bond lengths are 1.38 and 1.34 Å, respectively. These bond lengths differ from the transition state obtained for an isolated monoethyl zinc. The transition state is 1.15 eV above the initial structure. In the final configuration the remaining OH group of the water molecule is coordinated to two zinc atoms. The reaction is slightly endothermic with an energy change of 0.18 eV.

Cooperative Effects between Water Molecules. The lowest activation energy for the water pulse reactions calculated on the ethyl-saturated surface was 0.93 eV. There are several cases where the calculated barriers were very high, and thus the

event has a low probability of occurring. Therefore, in some instances it is possible that more water molecules adsorb onto the surface before the previous water molecule has reacted. To investigate the possible effect an additional water molecule might have on a surface reaction, two configurations with additional water molecules were studied.

First, a water molecule was introduced to the C1-5MEZ-1H₂O configuration. The water molecule was added onto the monoethyl zinc that served as the metastable adsorption site for the first water molecule as illustrated in Figure 4. We wanted to place the second molecule close to the first water molecule and study the effects that a new hydrogen bond can have as a point of principle. The second water molecule has an adsorption energy of -0.27 eV. The low adsorption energy of the additional water is likely due to steric hindrance because of the high surface ethyl concentration. Despite this weak bond energy, the molecule did not desorb during a molecular dynamics simulation, and we can consider this site at least a local minimum. With the water molecules close enough to form a hydrogen bond we can use the same mechanism as for the single water molecule.

The additional water molecule forms a hydrogen bond with the dissociated water molecule and stabilizes the transition state leading to a decrease in the activation energy from 1.15 to 0.91 eV. The reaction is exothermic with -0.92 eV. The C–H and O–H bond lengths in the transition state are 1.43 and 1.30 Å, respectively. The water–water interaction clearly has a stabilizing effect. However, the barrier for the ligand-exchange remains on par with the other mechanisms discussed.

Second, we performed calculations on the C1-1MEZ-5H₂O configuration in a similar fashion as the previous mechanisms; i.e., we placed a water molecule onto a suitable adsorption site on the surface and ran a short molecular dynamics simulation. The water molecule was placed on a bare surface zinc atom close to the MEZ where the adsorption energy for the water molecule was -0.75 eV. Unlike for the C1-5MEZ-2H₂O configuration, the adsorption bond of the additional water molecule is moderately strong. We calculated the reaction barrier for the same mechanism (same water molecule reacting from the same direction) as in the C1-1MEZ-5H₂O mechanism to compare the effect of the additional water. The reaction barrier decreased slightly from 1.22 to 1.14 eV. There is no direct interaction between the new water molecule and the reacting hydroxyl group, and hence the stabilizing effect is weaker than in the case of mechanism C1-5MEZ-2H₂O.

However, a reaction between the new water molecule and the monoethyl zinc was also investigated. This reaction had a considerably lower barrier of 0.72 eV. The main factor leading to the lowering of the reaction barrier is the more suitable direction of attack the new water molecule has. Unlike the three-coordinated hydroxyl group in the mechanism C1-1MEZ-5H₂O, the new water molecule is situated closer to the monoethyl zinc group on a zinc atom and has a more flexible structure because the oxygen is only one-coordinated.

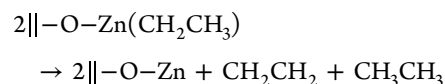
In conclusion, we find that additional water molecules have an effect on the surface kinetics by stabilizing the ligand-exchange mechanisms with additional hydrogen bonds or by attacking surface ethyl groups from the less constrained configuration when all the highly coordinated adsorption sites have been occupied by water molecules.

Pyrolysis and Radical Formation. The pyrolysis of ethyl groups was studied as an alternative route for ethyl elimination besides ligand-exchange with water. Two possible pyrolysis

mechanisms were investigated: formation of an ethyl radical as an intermediate species and a β -elimination type ethyl–ethyl pyrolysis reaction.

A free ethyl radical is a possible intermediate step in a pyrolysis reaction. Therefore, we studied the formation of a free radical on the isolated monoethyl zinc as well as on two saturated structures with low and high ethyl-densities, a C1-5MEZ-0H₂O configuration and a C2-1MEZ-4H₂O. In all the above cases, the formation of an ethyl radical on the surface had a barrier close to 3 eV, making any process where a free ethyl radical would be formed as an intermediate unlikely during the deposition process.

The β -elimination is a mechanism where one of the ethyl ligands donates a proton from the β -carbon to the α -carbon of another ligand resulting in the formation of ethane and ethene. Our calculations show this mechanism to also have a large barrier. We studied the elimination reaction on the C1-5MEZ-0H₂O structure as in this structure the ethyl concentration is the highest. The equation for the reaction can be written as



In order for the ethyl to accept the proton, the ligand almost has to become a free radical. This is evident from the Zn–C bond length that increases from 1.98 to 2.89 Å. The Zn–C bond length of the donating ligand remains close to the initial value and increases only slightly from 1.97 to 2.08 Å. The transition state is 2.52 eV above the initial state making the mechanism inaccessible at the usual process conditions.

DISCUSSION

A thorough investigation of surface reactions during the water pulse of the ALD of zinc oxide has been conducted on a complex ethyl-saturated surface. We summarize our central findings and present a schematic representation of the deposition process as a function temperature based on our *ab initio* calculations of the two ALD cycles.

The chemical environment of the surface after the diethyl zinc pulse is drastically different from a clean, hydroxylated surface before the pulse. The ethyl-covered surface has a very flexible structure with a vast number of potential energy minima. It becomes difficult, therefore, to be certain that a given structure is actually the energy minimum within a given basin. In this work we have tried to overcome this complexity by allowing the system to evolve into a preferred minimum energy structure using *ab initio* molecular dynamics. Several snapshots from the dynamical trajectories were optimized, and the lowest energy configuration was chosen as the starting point for a ligand-exchange reaction calculation. Thus, the initial structures chosen are reasonably close to a global minimum in a given basin and as such represent the configurations with large statistical weights. For any given initial structure, there are of course several possible reaction pathways for the system to choose from, and it is impossible to investigate all these possible pathways in a reasonable time. One or more pathways were tested, and the lowest activation energy from a set of calculations has been reported.

As the initial configurations are generated from an MD trajectory, it is not possible to control for different variables, for example, the coordination number of a monoethyl zinc group. Trying to vary different conditions leads to higher potential energy structures that cannot be considered as reasonable

starting positions. We have therefore restricted our investigation only to those configurations obtained from the molecular dynamics simulations. In all the mechanisms, a Lewis-basic water formed a bond with a Lewis acidic zinc atom as an intermediate before the ligand-exchange reaction.

The surface reactions investigated on the ethyl-saturated surface spanned a broad spectrum of reaction barriers ranging from 0.72 to 1.56 eV, i.e., from moderately high to inaccessible at the process conditions. As there are several possible reaction pathways, this list of surface reactions is by no means exhaustive but serves to present an overall range of activation energies for the water pulse ligand-exchange reactions. The lowest barriers reported here are considerably lower than those previously reported for DEZ/H₂O by Afshar and Cadien¹² on ZnO and by Ren¹³ on Si(100) using cluster models.

In a common *ab initio* study on the surface chemistry of atomic layer deposition, the reactive site is represented by an isolated atom/group on the surface.^{12–14,21–23} This type of model has considerably fewer degrees of freedom than a fully saturated surface, and the minimum energy structure is better defined. However, the complex surface environment due to the ligand-saturated surface is neglected. In order to compare the two approaches, we also studied the adsorption and ligand-exchange reaction of a water molecule on a single monoethyl zinc site.

The main difference between the simple and complex surface models was in the adsorption of the water onto the monoethyl zinc. The strength of the adsorption on the single monoethyl zinc site differs greatly from the adsorption on the ethyl-saturated surfaces. The bond energy on the isolated site is weak, only -0.36 eV, while on the saturated structures the adsorption bonds vary from -0.8 to -2.3 eV. The weak adsorption bond on the isolated MEZ site is also reflected by the lengthy Zn–O bond of 2.3 Å, which is considerably longer than on the saturated surfaces, where the adsorption bond is close to the bulk value of 2 Å, or even shorter. The monoethyl zinc groups clearly make the surface more susceptible to water adsorption, which is vital to the overall process. This type of cooperative effect by additional metal precursor fragments on the water adsorption has been previously reported by Shirazi and Elliott.²⁴

The barrier for the ligand-exchange reaction on the isolated monoethyl zinc site is on the same order as barriers on the saturated structures. The partial charges on the atoms involved in the ligand-exchange reaction (i.e., atoms part of the C–H–O transition state as well as the Zn atom), based on Hirshfeld analysis, are the same for the isolated monoethyl zinc as for all the calculations on the ethyl-saturated surface.

In addition to the cooperative effect that ethyl ligands have on the adsorption of water, our results show that water–water interactions have a cooperative effect in decreasing the reaction barriers for the water pulse reactions. In our two test cases, the barriers for the ligand removal decreased, from 1.15 to 0.91 eV and from 1.22 to 1.14 eV. We also investigated a reaction between an additional water molecule and the monoethyl zinc and found a low reaction barrier of 0.72 eV. This exceptionally low barrier was due to the flexible geometry of the water molecule in comparison with the highly coordinated surface hydroxyl group. There exists a linear trend between the adsorption energy of the water molecule and the activation energy of the ligand-exchange reaction. As the adsorption bond becomes stronger, the activation energy for the ligand-exchange reaction becomes larger. When the highly coordinated surface

sites have been saturated with water molecules, additional water may form weaker adsorption bonds and hence react with a lower barrier.

If we compare the activation energies for the water pulse with those reported for the diethyl zinc pulse,¹⁴ we can conclude that the ligand-exchange reactions during the water pulse have overall higher activation energies than during the diethyl zinc pulse. The relatively low barriers (<1 eV) are the processes that mainly contribute to the growth of the thin film as they are accessible in the process conditions. However, in most instances, especially in the case 2 saturated surface where bare zinc is present, the barrier for the ligand removal was large (>1 eV). While the water–water interaction can reduce these barriers, our calculations predict that some of the ligands on the surface may persist and cannot be removed, especially at low temperatures. Comparing the reaction barriers between the two precursor pulses, we estimate that the decrease in growth-per-cycle (GPC) of the growth process at low temperatures is due to the persistence of ethyl ligands at these temperatures.

This finding is supported by experiments conducted by Mackus et al.¹¹, where the authors observe that, in depositing zinc oxide, the surface ethyl-ligand elimination during the water pulse is incomplete, resulting in persisting ethyl ligands on the surface after the water pulse has ended. The fraction of these persisting ligands is strongly dependent on temperature, suggesting that there is a kinetic barrier to ligand elimination by water.

There is scarce experimental data to directly quantitatively compare our calculations. Holmqvist et al.⁹ have constructed a kinetic model for the DEZ/H₂O process. In their model, which is fitted to experimental QCM data, they present a barrier of 0.43 eV, which is close to the ligand-exchange barrier for diethyl zinc. However, this model has been constructed on the premise that all the ligands are removed between each reactant pulse, and it is unclear what kind of results a modification to this scheme would produce.

In a recent experimental study by Vandalon and Kessels²⁵ the authors report that the activation energy for the water pulse ligand-exchange reaction increases during the water pulse for the TMA/H₂O-process as the surface ligand-concentration decreases. This type of ligand-dependent surface kinetics has also been pointed out by Shirazi and Elliott.²⁴ We observe a weak trend between the surface ethyl concentration and the activation energy in our results. In our series of calculations, the barrier for the removal of the final ethyl ligand is very high (from 1.22 to 1.56 eV). If the calculated activation energies for the ligand-exchange reactions on the saturated surfaces at different ethyl concentrations presented in Table 1 are considered, there is a weak correlation between the activation energies and surface ethyl coverage in our calculations. If the calculations done on case 1 and case 2 surfaces are considered separately, the surface reactions on the case 1 surface have a moderate trend where the reaction barrier increases as the ethyl concentration decreases in agreement with Vandalon and Kessels. For the case 2 surface this trend is very weak.

At 0 K we do not observe any barrier for adsorption for a single water molecule at the highest ethyl concentration. However, the adsorption is weak for a subsequent water molecule at the high ethyl coverage due to steric effects. Thus, one may expect that the adsorption of several water molecules is inhibited at high ethyl coverages. The sensitivity of H₂O adsorption to the surface coverage likely leads to coverage-dependent initial surface kinetics.

Table 2. Reaction Rates for Different Activation Energies at Different Deposition Temperatures^a

example mechanism	E_a /eV	k_{50}/s^{-1}	k_{100}/s^{-1}	k_{150}/s^{-1}	k_{200}/s^{-1}
DEZ \rightarrow MEZ mechanism, LE1 ¹⁴	0.5	1×10^5	1×10^6	1×10^7	5×10^7
C1-1MEZ-6H ₂ O	0.7	8×10^1	3×10^3	4×10^4	3×10^5
C2-2MEZ-3H ₂ O/MEZ \rightarrow Zn, LE2 ¹⁴	0.9	6×10^{-2}	5×10^0	2×10^2	3×10^3
C1-5MEZ-1H ₂ O	1.1	5×10^{-5}	1×10^{-2}	7×10^{-1}	2×10^1
C2-1MEZ-4H ₂ O	1.5	3×10^{-11}	4×10^{-8}	1×10^{-5}	1×10^{-3}
H ₂ O adsorption	0.0	$1 \times 10^{4-6}$	$9 \times 10^{3-5}$	$9 \times 10^{3-5}$	$8 \times 10^{3-5}$
DEZ adsorption	0.0	$5 \times 10^{3-5}$	$4 \times 10^{3-5}$	$4 \times 10^{3-5}$	$4 \times 10^{3-5}$

^aThe example mechanisms shown roughly correspond to the given activation energy for which the reaction rate coefficients have been calculated. The temperatures are in °C. The adsorption rates range depending on the pressure of the precursor from 2 to 200 Pa. The reaction rates have been calculated using the Eyring equation and the adsorption rate from the particle flux from kinetic gas theory.^{21,26}

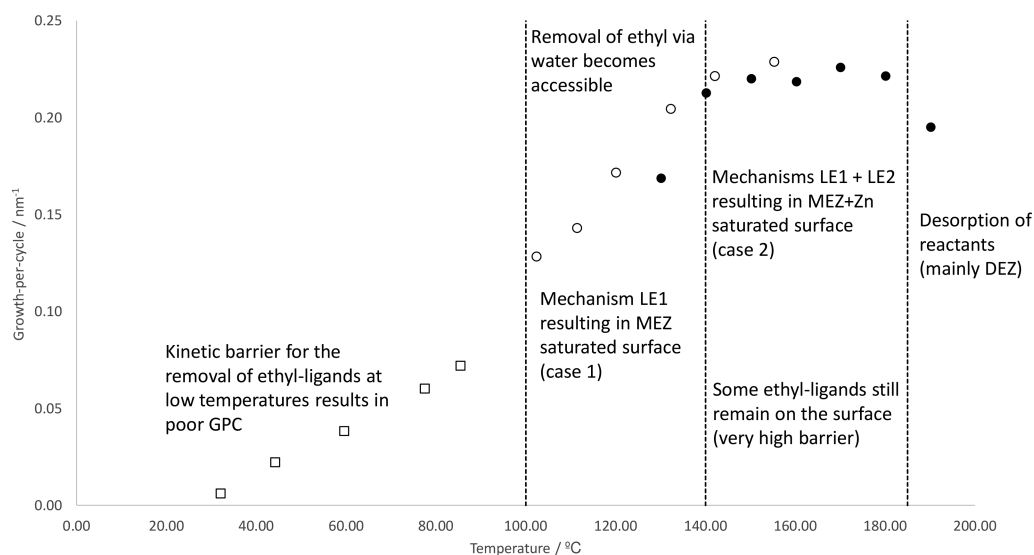


Figure 5. Growth-per-cycle (GPC) as a function of temperature adopted from Yousefi et al.⁸ with a schematic representation of the growth of ZnO thin films. Different symbols (empty squares, empty circles, black circles) correspond to different experimental runs. The LE1 and LE2 correspond to the DEZ and MEZ ligand-exchange reactions on the surface leading to MEZ and Zn, respectively. Case 1 and case 2 are the low and high temperature ethyl-saturated structures, respectively.

Pyrolysis of diethyl zinc into butane or other fragments has been proposed in the literature.¹⁰ The pyrolysis of DEZ at low surface ethyl coverage has previously been studied,¹⁴ and the barrier for pyrolysis was reported to be 1.96 eV. We looked at several possible pyrolysis mechanisms on the ethyl-saturated surface to see if this reaction pathway would be feasible at high ethyl concentrations. The mechanisms studied included the formation of a free ethyl radical as an intermediate species and a β -elimination mechanism between two ethyl ligands. These types of pyrolysis mechanisms have very large activation energies and are unlikely to contribute to the deposition of the zinc oxide thin films.

In Table 2 the reaction rates coefficients for different activation energies at different temperatures are presented, accompanied by an example mechanism corresponding roughly to that activation energy. The list of activation energies spans the range of reaction barriers we have calculated for the water pulse reactions and contains also the low barrier for the ligand-exchange of the diethyl zinc to monoethyl zinc as well as rates for adsorption of both water and diethyl zinc. We can now interpret the changes in the GPC with varying temperature from the insight gained from our *ab initio* calculations.

The deposition of the zinc oxide onto a hydroxylated zinc oxide surface begins with the diethyl zinc pulse. Diethyl zinc can react on the surface via two processes:¹⁴ the conversion of

diethyl zinc to monoethyl zinc (denoted LE1, barrier less than 0.5 eV) and the subsequent reaction of monoethyl zinc to bare zinc (denoted LE2, barriers ranging 0.95–1.52 eV). Both these processes require a proton from a surface group. It is evident from the rates in Table 2 that at every temperature the diethyl zinc can react on the surface to produce MEZ.

The water pulse kinetics are the rate-determining step in the overall process due to the relative size in the reaction barrier. The water ligand-exchange mechanism with the lowest barrier is slow but accessible even at 50–100 °C. However, all the other water pulse mechanisms have very low reaction rate coefficients. At elevated temperatures other mechanisms with higher barriers also become accessible. While it is evident that the mechanisms with the lowest barriers play an important part in the deposition process, our sample of mechanisms suggests that there exist several high barrier processes during the water pulse that are very sensitive to deposition temperature.

If one compares the rate coefficients with the adsorption rates, it is clear that the adsorption rate of new precursors is larger than the rate coefficient for most of the surface processes. This suggests that it is likely that, before a water molecule can react, another water molecule will adsorb nearby. If the surface ethyl coverage is not too high, the new molecule will form a relatively strong adsorption bond and water–water-interactions can help to stabilize the transition state and lower the reaction

barrier. The probability that a water–water interaction can help to stabilize a ligand-exchange reaction increases at extended exposures.

In many instances, however, the barriers for the ligand-exchange reactions are substantially high, even if lowered by cooperative effects. This leads to persisting ligands on the surface. These ligand-sites form defects into the lattice structure as the zinc is not saturated by oxygen and also produce impurities into the composition of the thin film as carbon and excess hydrogen is left in the substructure of the film. At elevated temperatures the kinetic barrier for the ligand removal is overcome, and the amount of persisting ligands can be expected to be reduced as a function of temperature. This is also what is observed experimentally.¹¹

We have summarized our conceptual view of the process in Figure 5 where we have roughly divided an experimental growth profile⁸ of the thin film into a few distinct blocks and characterized the atomic level processes contributing to the growth of the film. The removal of the first ligand from DEZ has a low barrier, and hence the surface is saturated with MEZ at all temperatures. At low temperatures the growth of the thin film is hindered due to the large kinetic barrier for the removal of the ethyl ligands on the surface. As the temperature increases, the removal of ethyl ligands becomes feasible, and the surface ethyl-saturation structure resembles that of the case 1 structure we have used in this paper, i.e., a surface where the saturation is due to steric hindrance of the ethyl ligands with several hydroxyl group present on the surface.

At elevated temperatures, some of the MEZ may react further to Zn (LE2). This decreases the steric repulsion between zinc precursor molecules and increases DEZ adsorption. This also creates further sites for water to adsorb to and increases the GPC. The resulting saturation structure corresponds to the case 2 structure discussed in this paper, where the saturation is limited by the amount of available protons on the surface as well as the steric repulsion between the ligands. At very high temperatures, desorption of the precursors starts to dominate, leading to a decrease in the overall GPC. Since the DEZ has a smaller adsorption energy (of -0.74 eV) than water in most of the configurations studied, it is likely that DEZ desorption is the limiting factor at high temperatures.

CONCLUSION

The atomic layer deposition of zinc oxide has been under intense research in the past few years. The surface reactions with the metal precursor, diethyl zinc, have been previously studied. However, to obtain a complete picture of the overall process, one must study the surface kinetics of both of the precursor pulses. In this paper we extend our previous computational study on the system to also include calculations on the water pulse reactions. We investigated the adsorption and ligand-exchange reactions of water on an isolated monoethyl zinc site, in the fashion of traditional single site surface calculations usually presented in the literature, as well as on ethyl-saturated surfaces that better represent the complex chemical environment of the surface after the diethyl zinc has saturated the surface. *Ab initio* molecular dynamics have been used to sample different configurations to obtain a minimum energy structure as an initial state for each surface reaction.

The calculations done on the ethyl-saturated surfaces are consistent in that the surface ligand-exchange reactions between water and ethyl ligands have a considerably higher barrier than

the surface reactions during a diethyl zinc pulse. The lowest calculated barriers for the water pulse reactions are accessible in the process conditions. However, in some instances the barriers for the removal of the ethyl ligand were very high, suggesting that some ethyl ligands may persist on the surface after the water pulse, which has recently been observed in experiments. We do not observe a clear dependency between the activation energies for the ligand-exchange reactions and the surface ethyl concentration. However, the adsorption of water at high ethyl coverages is inhibited due to steric effects.

The calculations for the isolated site differ from the calculations done on the saturated structures. The calculated reaction barrier for the ligand-exchange reaction between the water and the monoethyl zinc is in agreement with the calculations on the saturated surfaces. However, the adsorption energy for water on the isolated site does not agree with the calculations done on the ethyl-saturated surface. The bond between a single monoethyl zinc and a water molecule is extremely weak whereas on the saturated surface the water adsorption bond energies ranged from moderately to very strong. It is evident that a cooperative effect between the monoethyl zinc groups increases the adsorption of water onto the surface.

A cooperative effect is also demonstrated between the water molecules. Hydrogen-bond formation between adsorbants clearly has some stabilizing effect on the surface reactions; however, it is considerably lower than in some other cases reported.^{21,24,27} It is also observed that, after the under-coordinated adsorption sites have been saturated from the surface, water can occupy adsorption sites with lower coordination number. These less coordinated water molecules have a more flexible structure, and the ligand-exchange from these sites has a lower reaction barrier.

Possible pyrolysis pathways for ethyl ligands on the surface were also studied as pyrolysis has been suggested in the literature.¹⁰ Our calculations show no indication that pyrolysis of ethyl ligands would occur during the deposition process as all the considered mechanisms have very high activation energies.

In summary, we have presented a comprehensive computational study of the surface reactions for the water pulse of atomic layer deposition of zinc oxide. A large number of ligand-exchange reactions on the surface have been sampled, and the calculations are in good agreement with experimental data on the thin film growth. We have included a mechanistic interpretation of the DEZ/H₂O-process as a function of temperature and identified the crucial mechanisms that play a part in different regions. Quantum chemical methods are a useful tool to be used side-by-side with experiments in gaining an overall understanding of the growth process.

ASSOCIATED CONTENT

Supporting Information

The Supporting Information is available free of charge on the ACS Publications website at DOI: 10.1021/acs.jpcc.7b11469.

Description of xyz-format files (PDF)

Reaction mechanisms of calculations done on the ethyl-saturated surface and presented in Table 1 as trajectories in xyz-format (ZIP)

AUTHOR INFORMATION

Corresponding Author

*E-mail: kari.laasonen@aalto.fi.

ORCID 

Timo Weckman: 0000-0001-8721-560X

Kari Laasonen: 0000-0002-4419-7824

Notes

The authors declare no competing financial interest.

ACKNOWLEDGMENTS

The authors thank the Center for Scientific Computing for the use of their computational resources. Funding by the Academy of Finland (Project Nos. 13140115 and 13258547) and the Academy of Finland Centre of Excellence in Computational Nanoscience (Project No. 9158041) is acknowledged. We also thank Simon Elliott from the Tyndall National Institute, University College Cork, for very insightful and helpful discussions on interpreting the data in this article.

REFERENCES

- (1) Pinna, N.; Knez, M. *Atomic Layer Deposition of Nanostructured Materials*; Wiley-VCH, 2012.
- (2) Karpina, V.; Lazorenko, V.; Lashkarev, C.; Dobrowolski, V.; Kopylova, L.; Baturin, V.; Pustovoytov, S.; Karpenko, A. J.; Eremin, S.; Lytvyn, P.; et al. Zinc Oxide-Analogue of GaN with New Perspective Possibilities. *Cryst. Res. Technol.* **2004**, *39*, 980–992.
- (3) Morkoc, H.; Özgür, Ü. *Zinc Oxide: Fundamentals, Materials and Device Technology*; John Wiley & Sons, 2008.
- (4) Moezzi, A.; McDonagh, A. M.; Cortie, M. B. Zinc Oxide particles: Synthesis, Properties and Applications. *Chem. Eng. J.* **2012**, *185*, 1–22.
- (5) Yuan, N.; Wang, S.; Tan, C.; Wang, X.; Chen, G.; Ding, J. The Influence of Deposition Temperature on Growth Mode, Optical and Mechanical Properties of ZnO Films Prepared by the ALD Method. *J. Cryst. Growth* **2013**, *366*, 43–46.
- (6) Pung, S.-Y.; Choy, K.-L.; Hou, X.; Shan, C. Preferential Growth of ZnO Thin Films by the Atomic Layer Deposition Technique. *Nanotechnology* **2008**, *19*, 435609.
- (7) Tynell, T.; Karppinen, M. Atomic Layer Deposition of ZnO: A Review. *Semicond. Sci. Technol.* **2014**, *29*, 043001.
- (8) Yousfi, E. B.; Fouache, J.; Lincot, D. Study of Atomic Layer Epitaxy of Zinc Oxide by in-situ Quartz Crystal Microgravimetry. *Appl. Surf. Sci.* **2000**, *153*, 223–234.
- (9) Holmqvist, A.; Törndahl, T.; Magnusson, F.; Zimmermann, U.; Stenström, S. Dynamic Parameter Estimation of Atomic Layer Deposition Kinetics Applied to *in situ* Quartz Crystal Microbalance Diagnostics. *Chem. Eng. Sci.* **2014**, *111*, 15–33.
- (10) Ferguson, J.; Weimer, A.; George, S. Surface Chemistry and Infrared Absorbance Changes During ZnO Atomic Layer Deposition on ZrO₂ and BaTiO₃ Particles. *J. Vac. Sci. Technol., A* **2005**, *23*, 118–125.
- (11) Mackus, A. J.; MacIsaac, C.; Kim, W.-H.; Bent, S. F. Incomplete elimination of precursor ligands during atomic layer deposition of zinc-oxide, tin-oxide, and zinc-tin-oxide. *J. Chem. Phys.* **2017**, *146*, 052802.
- (12) Afshar, A.; Cadien, K. C. Growth Mechanism of Atomic Layer Deposition of Zinc Oxide: A Density Functional Theory Approach. *Appl. Phys. Lett.* **2013**, *103*, 251906.
- (13) Ren, J. Initial Growth Mechanism of Atomic Layer Deposition of ZnO on the Hydroxylated Si (100)-2×1: A Density Functional Theory Study. *Appl. Surf. Sci.* **2009**, *255*, 5742–5745.
- (14) Weckman, T.; Laasonen, K. Atomic Layer Deposition of Zinc Oxide: Diethyl Zinc Reactions and Surface Saturation from First-Principles. *J. Phys. Chem. C* **2016**, *120*, 21460–21471.
- (15) Enkovaara, J.; Rostgaard, C.; Mortensen, J.; Chen, J.; Dulak, M.; Ferrighi, L.; Gavnholt, J.; Glinsvad, C.; Haikola, V.; Hansen, H. Electronic structure calculations with GPAW: a real-space implementation of the projector augmented-wave method. *J. Phys. Condens. Matter* **2010**, *22*, 253202–253225.
- (16) Perdew, J. P.; Burke, K.; Ernzerhof, M. Generalized Gradient Approximation Made Simple. *Phys. Rev. Lett.* **1996**, *77*, 3865.
- (17) Meyer, B.; Marx, D.; Dulub, O.; Diebold, U.; Kunat, M.; Langenberg, D.; Wöll, C. Partial Dissociation of Water Leads to Stable Superstructures on the Surface of Zinc Oxide. *Angew. Chem., Int. Ed.* **2004**, *43*, 6641–6645.
- (18) Calzolari, A.; Catellani, A. Water adsorption on nonpolar ZnO (1010) surface: A microscopic understanding. *J. Phys. Chem. C* **2009**, *113*, 2896–2902.
- (19) Tkatchenko, A.; Scheffler, M. Accurate Molecular van der Waals Interactions from Ground-state Electron Density and Free-atom Reference Data. *Phys. Rev. Lett.* **2009**, *102*, 073005.
- (20) Henkelman, G.; Uberuaga, B. P.; Jónsson, H. *J. Chem. Phys.* **2000**, *113*, 9901–9904.
- (21) Weckman, T.; Laasonen, K. First Principles Study of the Atomic Layer Deposition of Alumina by TMA-H₂O-process. *Phys. Chem. Chem. Phys.* **2015**, *17*, 17322–17334.
- (22) Elliott, S. D. Atomic-scale Simulation of ALD Chemistry. *Semicond. Sci. Technol.* **2012**, *27*, 074008.
- (23) Elliott, S. D.; Dey, G.; Maimaiti, Y.; Ablat, H.; Filatova, E. A.; Fomengia, G. N. Modeling Mechanism and Growth Reactions for New Nanofabrication Processes by Atomic Layer Deposition. *Adv. Mater.* **2016**, *28*, 5367–5380.
- (24) Shirazi, M.; Elliott, S. D. Cooperation Between Adsorbates Accounts for the Activation of Atomic Layer Deposition Reactions. *Nanoscale* **2015**, *7*, 6311–6318.
- (25) Vandalon, V.; Kessels, W. Revisiting the growth mechanism of atomic layer deposition of Al₂O₃: A vibrational sum-frequency generation study. *J. Vac. Sci. Technol., A* **2017**, *35*, 05C313.
- (26) Atkins, P. W.; De Paula, J. *Physical Chemistry*; Oxford University Press: Oxford, 2010; p 917.
- (27) Mukhopadhyay, A. B.; Musgrave, C. B.; Sanz, J. F. Atomic Layer Deposition of Hafnium Oxide from Hafnium Chloride and Water. *J. Am. Chem. Soc.* **2008**, *130*, 11996–12006.